ChemComm

Acetic Acid from CO_2, CH_3I and H_2 by Means of a Water-Soluble Electron Storage Catalyst

Journal:	*ChemComm*
Manuscript ID	CC-COM-03-2021-001611.R1
Article Type:	Communication

SCHOLARONE™
Manuscripts

Please do not adjust margins

COMMUNICATION

Acetic Acid from CO_2, CH_3I and H_2 by Means of a Water-Soluble Electron Storage Catalyst †

Received 00th January 20xx,
Accepted 00th January 20xx

DOI: 10.1039/x0xx00000x

Takeshi Yatabe,[a,b] Kazuki Kamitakahara,[a] Kaede Higashijima,[a] Tatsuya Ando,[a,b] Takahiro Matsumoto,[a,b] Ki-Seok Yoon,[a,b] Takao Enomoto[c] and Seiji Ogo*[a,b]

This paper reports a possible mechanism of acetic acid formation from CO_2, CH_3I and H_2, in aqueous media and central role played by a water-soluble Rh-based electron storage catalyst. In addition to the water-solubility, we also report crystal structures of two presumed intermediates. These findings together indicate: (1) the advantage of water, not only as a green solvent, but also as a reactive Lewis base to extract the H^+ from H_2, (2) the role of metal (Rh) centre as a point for storing electrons from H_2 and (3) the importance of an electron-withdrawing ligand (quaterpyridine, qpy) that supports the electron storage.

In nature, the enzyme [NiFe]hydrogenase extracts electrons from H_2 in water and transfers the extracted electrons to various terminal electron acceptors.[1] This ability of natural organisms to make use of H_2 in water is clearly of much interest to us, since it provides not only the potential for using H_2 as an electron donor in water, but also a means of synthesising organic feedstocks when combined with CO_2 as an electron acceptor. Needless to say, the ability to make use of CO_2 for commercial synthesis would prove a major boon to both the economy and the environment.[2] Therefore, [NiFe]hydrogenase could provide guidance into the development of catalysts that use H_2 as a source of electrons in water.

One example of using H_2 to produce a feedstock from CO_2 has been reported by Qian and coworkers.[3a,b] They used a mixture of CO_2, CH_3OH, H_2 and a Rh-based catalyst in organic solvents to produce acetic acid as an alternative to Monsanto process.[3c] Though this finding represents an important step in the field, no reaction mechanism has been identified.

In order to make significant advances on this topic the systematic development of H_2-activation catalysts is required, and this has been promoted in our lab by development of [NiFe]hydrogenase-mimic catalysts.[4] Indeed, these studies have enabled us to elucidate two important principles for the activation of H_2: (1) using water is not only a green solvent but, as a Lewis base, it is able to extract the protons from a metal-bound H_2, leaving behind the electrons and (2) the reduced metal centre thus created must be combined with electron-withdrawing ligands that delocalise the extra electron density.[5]

In this paper, we not only report the synthesis of acetic acid from CO_2 and CH_3I using H_2, but we perform the reaction in aqueous media. Furthermore, we present crystal structures of a Rh complex with two intermediates, allowing us to have confidence in a detailed reaction mechanism with central requirements for the catalyst design.

A Rh^{III} dichloride complex $[Rh^{III}(qpy)Cl_2](Cl)$ {[**1**](Cl), qpy = 2,2':6',2":6",2"'-quaterpyridine} was synthesised by the reaction of $Rh^{III}Cl_3$ with qpy in ethanol under reflux conditions. Subsequently, it was characterised by X-ray analysis (Fig. 1, Table S1, ESI), electrospray ionization mass spectrometry (ESI-MS, Fig. S1, ESI), ^1H NMR spectroscopy (Fig. S2, ESI) and elemental analysis. A single crystal of **1** suitable for X-ray analysis was obtained from the ethanol solution of **1**. An ORTEP drawing of **1** is depicted in Fig. 1. The Rh metal centre adopts a distorted octahedral geometry, in which the qpy ligand occupies equatorial sites and two chloride ions are coordinated at axial sites. The positive-ion ESI mass spectrum shows the prominent peak of *m/z* 483.1 {relative intensity (*I*) = 100 % in the range of *m/z* 100–2000} corresponds to a characteristic distribution that matched well with the calculated isotopic distribution of $[\mathbf{1}]^+$ (Fig. S1). The ^1H NMR signals were observed in the aromatic region, which are assigned to the protons of the qpy ligand (Fig. S2).

[a] *Department of Chemistry and Biochemistry, Graduate School of Engineering, Kyushu University*
International Institute for Carbon-Neutral Energy Research (WPI-I2CNER), Kyushu University,
744 Moto-oka, Nishi-ku, Fukuoka 819-0395 (Japan)
E-mail: ogo.seiji.872@m.kyushu-u.ac.jp.
[b] *Center for Small Molecule Energy, Kyushu University, 744 Moto-oka, Nishi-ku, Fukuoka 819-0395 (Japan).*
[c] *Specialty Chemicals Section, Technology Development Department, Technical Division, Tanaka Kikinzoku Kogyo K. K. 22 Wadai, Tsukuba, Ibaraki, 300–4247 (Japan).*

†Electronic Supplementary Information (ESI) available: [Experimental details, Table S1 and Figs. S1–S11.]. CCDC 2054176, 2054177 and 2054178. For ESI and crystallographic data in CIF or other electronic format see DOI: 10.1039/x0xx00000x

Please do not adjust margins

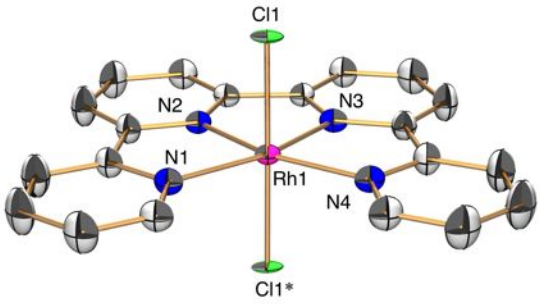

Fig. 1 An ORTEP drawing of [**1**](Cl) with the ellipsoids at 50% probability. Counteranion (Cl), solvents (H_2O) and hydrogen atoms are omitted for clarity. Selected interatomic distances (*l*/Å) and angles (ϕ/deg): Rh1–Cl1 = 2.3272(10), Rh1–N1 = 2.080(6), Rh1–N2 = 1.931(5), Rh1–N3 = 1.940(5), Rh1–N4 = 2.081(6), N1–Rh1–N4 = 118.1(2), N2–Rh1–N3 = 82.6(2), N1–Rh1–N2 = 79.6(2), N3–Rh1–N4 = 79.6(2).

Complex **1** reacts with H_2 (0.1 MPa) in water (pH 2.0–10) at room temperature to yield a water-soluble low-valent Rh^{I} complex [Rh^{I}(qpy)](Cl) {[**2**](Cl)}. Two electrons of H_2 are transferred to the Rh centre, which is facilitated by the electron-withdrawing effect of qpy to stabilise the low-valence of the Rh^{I} centre. The water used as the solvent can also accelerate this reaction due to the abstraction of protons from the original H_2.[5d]

Complex **2** was characterised by spectroscopic and mass spectrometric methods such as X-ray analysis (Fig. 2), ESI-MS (Fig. S3, ESI), UV-vis-NIR absorption spectroscopy (Fig. S4, ESI), X-ray photoelectron spectroscopy (XPS, Fig. S5, ESI) and elemental analysis. Exchanging the counteranion of Cl^- with $CF_3SO_3^-$ afforded a dark crystal of [**2**](CF_3SO_3) suitable for X-ray analysis (Fig. 2). This analysis showed that the two-electron reduction of the Rh^{III} centre to Rh^{I} led to a structural change from an octahedral to a square-planar geometry, which is ascribed to a d^8 low-spin configuration.[6] The positive-ion ESI mass spectrum of **2** shows a prominent peak of *m*/*z* 413.0 (*I* = 100 % in the range of *m*/*z* 100–2000). The signal has a characteristic isotopic distribution corresponds to the calculated isotopic distribution of [**2**]$^+$ (Fig. S3). The UV-vis-NIR absorption spectrum of **2** shows broad absorption bands over 600–1200 nm (Fig. S4), with features previously observed in the absorption spectra of Rh^{I} polypyridyl complexes.[7] In the XP (X-ray photoelectron) spectrum of **2** (Fig. S5), binding energies of 306.8 and 311.5 eV were observed for Rh $3d_{3/2}$ and $3d_{5/2}$, respectively, which are lower than those of Rh^{III} complex **1** (309.2 and 313.9 eV). These results indicate complex **2** adopts the univalent Rh centre.[8]

The Rh^{I} complex, **2**, can react with CH_3I to generate a water-soluble Rh^{III} methyl iodide complex [Rh^{III}(qpy)(CH_3)I](I) {[**3**](I)} in water (pH 2.0–10). The oxidative addition of CH_3I to Rh^{I} in this process means that two electrons originally acquired from H_2 are transferred to the CH_3I via the Rh centre.

Characterisation of **3** was conducted by X-ray analysis (Fig. 3), ESI-MS (Fig. S6, ESI), ^{1}H NMR spectroscopy (Fig. S7, ESI) and

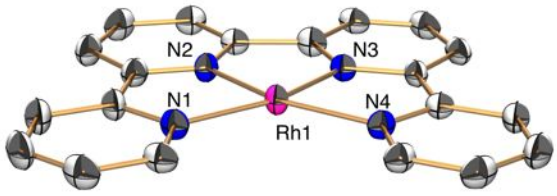

Fig. 2 An ORTEP drawing of [**2**](CF_3SO_3) with the ellipsoids at 50% probability. Counteranion (CF_3SO_3) and hydrogen atoms are omitted for clarity. Selected interatomic distances (*l*/Å) and angles (ϕ/deg): Rh1–N1 = 2.081(4), Rh1–N2 = 1.929(4), Rh1–N3 = 1.931(4), Rh1–N4 = 2.082(4), N1–Rh1–N4 = 118.95(18), N2–Rh1–N3 = 81.93(18), N1–Rh1–N2 = 79.54(18), N3–Rh1–N4 = 79.58(17).

elemental analysis. The addition of CH_3I to an aqueous solution of **2** resulted in the disappearance of the absorption band over 400 nm as monitored by UV-vis-NIR absorption spectroscopy (Fig. S8, ESI). A single crystal of [**3**](PF_6) was obtained from the acetonitrile solution of **3** diffused by diethyl ether with exchanging of the counterion from I^- to PF_6^-. The ORTEP drawing of [**3**](PF_6) clearly indicates that methyl and iodide ligands, originating from CH_3I, are coordinated to the Rh centre. The Rh metal centre adopts a distorted octahedral geometry composed of the methyl ligand, the iodide ion and the qpy ligand (Fig. 3). The Rh1–C1 distance {2.094(5) Å} is similar to those of the other Rh^{III} methyl complexes {2.015(5)–2.047(7) Å}.[9] The positive-ion ESI mass spectrum of *in-situ* solution shows the prominent peak of *m*/*z* 554.9 (*I* = 100 % in the range of *m*/*z* 100–2000), which has a characteristic isotopic distribution that matches well with the calculated isotopic distribution of [**3**]$^+$ (Fig. S6). The ^{1}H NMR spectrum of **3** shows a doublet peak at 0.79 ppm with a coupling constant of 2 Hz (Fig. S7). This is the expected pattern arising from the spin−spin interaction of the methyl protons with the Rh^{III} centre, which also possesses a nuclear spin of 1/2.

Having followed the stepwise reactions of **1** with H_2 and **2** with CH_3I, we conducted the final step of reacting **3** with CO_2. Complex **3** was reacted with CO_2 (0.8 MPa) in water at pH 2.0 and at 80 °C for 12 h. This process successfully produces acetic acid in a yield of 12%, based on [**3**](I) as quantified by high performance liquid chromatography (HPLC) (Fig. S9, ESI). These reactions separately demonstrated the successful stepwise employment of electrons from H_2 to activate CH_3I and reduce CO_2, thereby generating acetic acid in water.

The positive-ion ESI mass spectrum of the *in-situ* solution of **3** with CO_2 demonstrates the prominent peak at *m*/*z* 666.9 (*I* = 100 % in the range of *m*/*z* 100–2000) corresponding to the expected isotopic distribution. It matches well with the calculated distribution of a Rh^{III} diiodide complex [Rh^{III}(qpy)I_2]$^+$ (**4**), that is an iodide derivative of complex **1** (Fig. S10, ESI). These results clearly indicate the insertion of CO_2 to Rh–C bond of **3** followed by protonation to yield acetic acid.

This journal is © The Royal Society of Chemistry 20xx

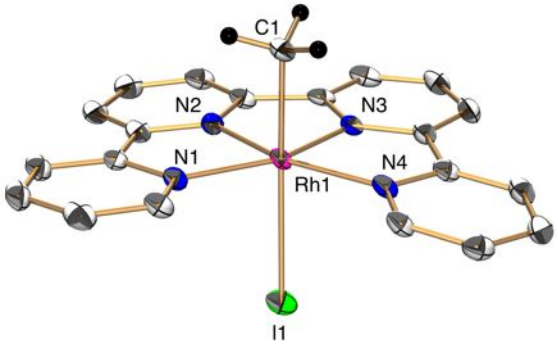

Fig. 3 An ORTEP drawing of [**3**](PF_6) with the ellipsoids at 50% probability. Counteranion (PF_6), solvent (acetonitrile) and hydrogen atoms of qpy are omitted for clarity. Selected interatomic distances (*l*/Å) and angles (ϕ/deg): Rh1–C1 = 2.094(5), Rh1–I1 = 2.8026(8), Rh1–N1 = 2.084(4), Rh1–N2 = 1.928(4), Rh1–N3 = 1.938(4), Rh1–N4 = 2.079(4), N1–Rh1–N4 = 118.94(16), N2–Rh1–N3 = 81.98(18), N1–Rh1–N2 = 79.57(17), N3–Rh1–N4 = 79.49(17).

Having established the stepwise reactions, we examined the catalytic property of **1** in the production of acetic acid from H_2, CO_2 and CH_3I in the presence of LiBr as a Lewis acid. The reaction was performed under H_2 (0.15 MPa) and CO_2 (0.8 MPa) at 80 °C for 24 h in H_2O/CH_3OH (1/1) at pH 2.0. The formed acetic acid was detected by gas chromatography mass spectrometry and quantified by HPLC, and the maximum turnover number (TON) was estimated at 1 (TON, mol of acetic acid/mol of complex **1**) (Fig. S11, ESI). No acetic acid was formed without **1**, H_2, CO_2 or CH_3I. Carbon monoxide was not produced under the reaction conditions, which was analysed by Gas chromatography. After one turnover, complexes **3** and **4** were present in solution. An isotope-labelled experiment using $^{13}CH_3I$ was performed, which produced $^{13}CH_3COOH$, indicating that the origin of CH_3 group is CH_3I (Fig. S11). Though the turnover was disappointing, this reaction demonstrated the feasibility of such a catalytic cycle in aqueous media.

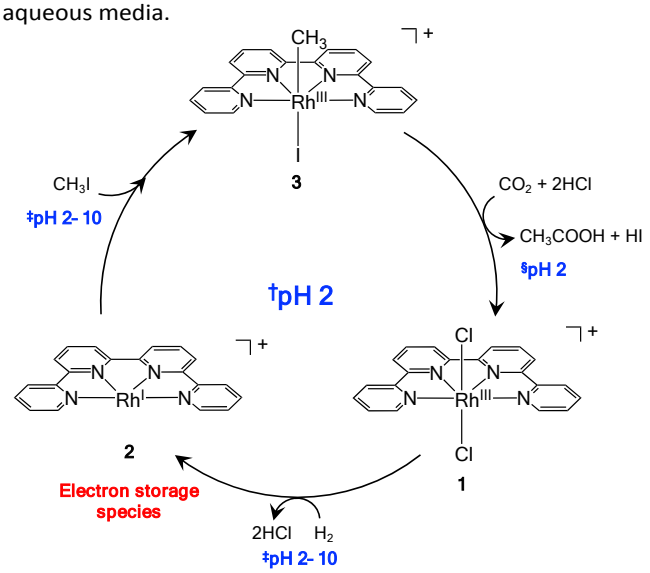

Fig. 4 A proposed reaction mechanism of the acetic acid formation from CO_2, CH_3I and H_2. † The catalytic reaction was carried out in H_2O/CH_3OH (1/1) at pH 2. Complexes **1**, **2** and **3** are stable at pH 2 under the catalytic conditions. ‡ The stepwise reactions from **1** to **2** and from **2** to **3** were carried out in water at pH 2-10. § The stepwise reaction from **3** to **1** was carried out in water at pH 2. No formation of acetic acid was observed above pH 3.

Given the above results, we have proposed the reaction mechanism as shown in Fig. 4. The water-soluble Rh^{III} complex **1** reacts with H_2 in water to form the water-soluble low-valent Rh^{I} complex **2** that can store two electrons from H_2. In the H_2 activation process, protons are abstracted from H_2 by the Lewis basicity of the water solvent. The reductive activation of CH_3I by the Rh^{I} centre of **2** then leads to the methyl- and iodide-coordinated water-soluble Rh^{III} complex **3**. Finally, insertion of CO_2 into Rh–C bond of **3**, followed by protonation, yields acetic acid. In summary, the water-soluble Rh qpy complex makes it possible to transfer the electrons from H_2 to CH_3I and CO_2 in water.

In conclusion, we have demonstrated the rational design of a water-soluble complex for the synthesis of acetic acid from CO_2, CH_3I and H_2 in aqueous media. This design confirms our long-standing confidence in the advantages of water solubility, metal centre as a point for storing electrons from H_2, and electron-withdrawing ligand. Though the performance of the complex requires further optimisation, it is the first example of such a complex that can work in aqueous media.

This work was supported by JST CREST Grant Number JPMJCR18R2, Japan, JSPS KAKENHI Grant Numbers JP26000008 (Specially Promoted Research) and JP19K05503.

Conflicts of interest

There are no conflicts to declare.

Notes and references

1 W. Lubitz, H. Ogata, O. Rüdiger, E. Reijerse, *Chem. Rev.* 2014, **114**, 4081–4148.
2 (a) T. Sakakura, J.-C. Choi, H. Yasuda, *Chem. Rev.* 2007, **107**, 2365–2387; (b) M. Cokoja, C. Bruckmeier, B. Rieger, W. A. Herrmann, F. E. Kühn, *Angew. Chem. Int. Ed.* 2011, **50**, 8510–8537.
3 (a) Q. Qian, J. Zhang, M. Cui, B. Han, *Nat. Commun.* 2016, **7**, 11481; (b) M. Cui, Q. Qian, J. Zhang, C. Chen, B. Han, *Green Chem.* 2017, **19**, 3558–3565; (c) X. Wang, Y. Yang, T. Wang, H. Zhong, J. Cheng, F. Jin, *ACS Sustainable Chem. Eng.* 2021, **9**, 1203–1212.
4 (a) D. Schilter, J. M. Camara, M. T. Huynh, S. Hammes-Schiffer, T. B. Rauchfuss, *Chem. Rev.* 2016, **116**, 8693–8749; (b) B. C. Manor, T. B. Rauchfuss, *J. Am. Chem. Soc.* 2013, **135**, 11895–11900; (c) T. Liu, D. L. DuBois, R. M. Bullock, *Nat. Chem.* 2013, **5**, 228–233; (d) D. Brazzolotto, M. Gennari, N. Queyriaux, T. R. Simmons, J. Pécaut, S. Demeshko, F. Meyer, M. Orio, V. Artero, C. Duboc, *Nat. Chem.* 2016, **8**, 1054–1060; (e) P. Ghosh, S. Ding, R. B. Chupik, M. Quiroz, C.-H. Hsieh, N.

Bhuvanesh, M. B. Hall, M. Y. Darensbourg, *Chem*. *Sci*. 2017, **8**, 8291–8300.

5 (a) S. Ogo, R. Kabe, K. Uehara, B. Kure, T. Nishimura, S. C. Menon, R. Harada, S. Fukuzumi, Y. Higuchi, T. Ohhara, T. Tamada, R. Kuroki, *Science* 2007, **316**, 585–587; (b) S. Ogo, K. Ichikawa, T. Kishima, T. Matsumoto, H. Nakai, K. Kusaka, T. Ohhara, *Science* 2013, **339**, 682–684; (c) S. Ogo, *Chem*. *Rec*. 2014, **14**, 397–409; (d) S. Ogo, *Coord*. *Chem*. *Rev*. 2017, **334**, 43–53; (e) S. Ogo, T. Kishima, T. Yatabe, K. Miyazawa, R. Yamasaki, T. Matsumoto, T. Ando, M. Kikkawa, M. Isegawa, K.-S. Yoon, S. Hayami, *Sci. Adv.* 2020, **6**, eaaz8181.

6 (a) R. Mathieu, G. Esquius, N. Lugan, J. Pons, J. Ros, *Eur*. *J*. *Inorg*. *Chem*. 2001, 2683–2688; (b) B. C. De Pater, H.-W. Frühauf, K. Vrieze, R. De Gelder, E. J. Baerends, D. McCormack, M. Lutz, A. L. Spek, F. Hartl, *Eur*. *J*. *Inorg*. *Chem*. 2004, 1675–1686; (c) D. Inoki, T. Matsumoto, H. Hayashi, K. Takashita, H. Nakai, S. Ogo, *Dalton Trans*. 2012, **41**, 4328–4334; (d) J. J. Gair, Y. Qiu, N. H. Chan, A. S. Filatov, J. C. Lewis, *Organometallics* 2017, **36**, 4699–4706; (e) S. Ogo, L. T. T. Minh, T. Kikunaga, T. Ando, T. Matsumoto, T. Yatabe, K. Kato, *Organometallics* 2020, **39**, 3731–3741.

7 (a) A. K.-W. Chan, K. M.-C. Wong, V. W.-W. Yam, *J*. *Am*. *Chem*. *Soc*. 2015, **137**, 6920–6931; (b) A. K.-W. Chan, D. Wu, K. M.-C. Wong, V. W.-W. Yam, *Inorg*. *Chem*. 2016, **55**, 3685–3691; (c) A. K.-W. Chan, M. Ng, K.-H. Low, V. W.-W. Yam, *J*. *Am*. *Chem*. *Soc*. 2018, **140**, 8321–8329.

8 (a) Y. Okamoto, N. Ishida, T. Imanaka, S. Teranishi, *J*. *Cat*. 1979, **58**, 82–94; (b) K. J. Stanger, Y. Tang, J. Anderegg, R. J. Angelici, *J*. *Mol*. *Cat*. *A* 2003, **202**, 147–161.

9 (a) S. Nückel, P. Burger, *Organometallics* 2001, **20**, 4345–4359; (b) D. Cuervo, J. Díez, M. P. Gamasa, J. Gimeno, *Organometallics* 2005, **24**, 2224–2232.

This journal is © The Royal Society of Chemistry 20xx